Quality and Productivity Driven Trajectory Optimisation for Robotic Handling of Compliant Sheet Metal Parts in Multi-Press Stamping Lines

Emile Glorieux[a,*], Pasquale Franciosa [b], Darek Ceglarek [b]

[a] *Department of Engineering Science, University West, S-461 32 Trollhättan, Sweden*
[b] *Warwick Manufacturing Group (WMG), University of Warwick, CV4 7AL Coventry, United Kingdom*

Abstract

This paper investigates trajectory generation for multi-robot systems that handle compliant parts in order to minimise deformations during handling, which is important to reduce the risk of affecting the part's dimensional quality. An optimisation methodology is proposed to generate deformation-minimal multi-robot coordinated trajectories for predefined robot paths and cycle-time. The novelty of the proposed optimisation methodology is that it efficiently estimates part deformations using a precomputed Response Surface Model (RSM), which is based on data samples generated by Finite Element Analysis (FEA) of the handled part and end-effector. The end-effector holding forces, plastic part deformations, collision-avoidance and multi-robot coordination are also considered as constraints in the optimisation model. The optimised trajectories are experimentally validated and the results show that the proposed optimisation methodology is able to significantly reduce the deformations of the part during handling, i.e. up to 12% with the same cycle-time in the case study that involves handling compliant sheet metal parts. This investigation provides insights into generating specialised trajectories for material handling of compliant parts that can systematically minimise part deformations to ensure final dimensional quality.

Keywords: trajectory optimisation, multi-robot coordination, robotic material handling, compliant parts

1. Introduction

In manufacturing, an important issue involving compliant parts is maintaining dimensional quality by avoiding large deformations during the handling operations. Plastic part deformations must obviously be avoided since these would permanently deform it. Furthermore, even elastic deformations can deteriorate dimensional quality. Large elastic deformations can cause part distortions, due to an unevenly distributed contact force when it is dropped onto the surface at the place location [1]. Another issue involving large elastic part deformations are positioning errors of the part at the place location. The resulting positional variations are often problematic for product quality in manufacturing scenarios, for example when placing sheet metal parts into a die for stamping [1].

The magnitude of part deformations is influenced by the design of the end-effector that grips the part for the material handling operation, as this determines how the part is held/supported. This relationship has been investigated in previous research work. For example, Ceglarek et al. [2] propose a methodology for end-effector design optimisation to minimise part deformations during handling. The modelling of the end-effector was further improved by Li et al. [1] to overcome the shortcomings with rigid point part-holding modelling of the end-effector which results in more reliable deformation predictions by using a dexterous end-effector part-holding model. Furthermore, Hoffmann and Kohnhäuser [3] propose a methodology to optimise the vacuum-cups' positions for end-effectors handling sheet metal plates in crossbar transfer press in order to improve the productivity, reduce the holding force and the part deformations.

However, robot path and trajectory can also influence part deformations since these determine the motion of the end-effector holding the handled part and consequently, the forces acting on the part such as acceleration-induced inertia and drag. In other words, changes to the robot trajectory will affect part deformations and thereby, potentially also its final dimensional quality due to plastic deformations as well as distortions and positioning variations when dropping the (elastically) deformed part at the place location. A survey of model-based manipulation planning of deformable objects is given by Jiménez [13]. As can be seen that there is a paucity of research on planning robot paths and/or trajectories to reduce deformations during handling. A deformation minimal robot trajectory can be obtained by avoiding sharp/high accelerations and consequently avoid large inertia forces as well as high speeds that cause large drag forces. For a single robot system, there is thus, a straightforward relationship between the magnitude of part deformations and the system's cycle-time. However, industrial material handling robots are often situated in multi-robot systems, i.e. there are multiple robots (or obstacles) moving simultaneously in the same workspace. In such multi-robot systems, there are additional constraints for the robot trajectories concerning the multi-robot coordination necessary to avoid collisions between the robots, which, in turn, also influences the system's cycle-

*Corresponding author
Email address: emile.glorieux@hv.se (Emile Glorieux)

Table 1: Review and research directions in trajectory optimisation for robotic handling of rigid and compliant objects

	Material handling system elements				Part modelling		
	Robot-system		End-effector		Rigid	Non-rigid	
	Single-robot	Multi-robot	Rigid	Non-rigid		2.5D	3D
Li and Ceglarek [4]				x		x	
Aomura et al. [5] Belchior et al. [6] Opritescu and Volk [7]	x		x		x		
Glorieux et al. [8]		x	x		x		
Proposed in this paper		x	x			x	
Potential synergies	↕	↕		↕			↕
Dexterous robot hands Okamura et al. [9] Bicchi and Kumar [10] Butterfass et al. [11]				x			x
Soft robotics Russ and Tolley [12]	x						

time. The relationship between the magnitude of part deformations and the system's cycle is thus more intricate for multi-robot systems. It thereby becomes challenging to generate robot trajectories that minimise the deformation of the handled parts due to the forces resulting from the motions of the robot end-effector, while simultaneously planning the multi-robot coordination for avoiding collisions between the robots and meeting the required cycle-time for the multi-robot system.

A typical application where this issue is relevant is the material handling of compliant sheet metal parts, which occurs in several manufacturing industries, e.g. automotive, aerospace, appliances, etc. The dimensional quality of the sheet metal parts is usually a critical aspect. The robot motion planning for these material handling systems commonly either ignores the part deformations by assuming that the handled compliant parts are rigid, or focusses on avoiding only plastic deformations. The former was found to be the case through work by Glorieux et al. [14, 8], which investigated multi-robot motion planning for material handling of sheet metal parts in order to improve productivity and reduce robot wear. The same assumption ("rigid-parts") is made in other studies concerning designing the tool paths, bending sequences and motions for robotic sheet metal part forming [5, 15, 6, 7]. Assuming that the handled compliant parts are rigid ignores that the deformations during handling can affect the final dimensional quality.

Li and Ceglarek [4] proposed a methodology for time-optimised path planning and trajectory generation for handling compliant sheet metal parts with consideration to avoid plastic part deformations during handling. The methodology focussed on minimising the execution-time for the material handling operation while avoiding plastic deformations of the handled parts, thereby allowing large elastic deformations. However, only the path and trajectory for the end-effector to transfer the part is planned, and not the robot motion in terms of the robot joints to move the end-effector according to the planned path and trajectory, thereby neglecting the robot kinematics/dynamics. These characteristics, together with the fact that only a single isolated material handling operation is considered, severely limits the methodology rendering it inapplicable to multi-robot systems for material handling of compliant parts. Recent research by Glorieux et al. [16] proposes optimising the end-effector design co-adaptively with the robot motion planning to primarily improve productivity, and next minimise part deformations. Results showed a significant improvement in productivity of the robotic material handling system. The robot trajectories are however generated according to the logic of the supplier-provided robot controller, whereas specific tailored trajectories for each motion can potentially reduce part deformations even further.

As it was suggested by one of the paper reviewers, currently, the flexible grippers (dexterous hand) fitting the shape of objects have not been designed and used for the stamping press applications. However, we feel that there are potential synergy between research in trajectory planning used for multi-robot handling of compliant sheet metal parts [4, 16], and research in the area of dexterous robot hands [9, 6, 10], For example, the application of multi-robot handling of textiles and food products which are highly variable both in shape, size and structure can benefit from integrating trajectory planning work presented in this paper with work conducted in the area of dexterous robot hands design. Table 1 presents these potential synergies in the form of review and research direction in the area of trajectory planning for robotic handling of rigid and compliant objects.

This paper specifically aims to investigate reducing part deformation during handling by optimising the coordinated robot trajectories in order to ensure final dimensional quality. A novel optimisation methodology to generate deformation-minimal trajectories is proposed that integrates deformation modelling of the handled parts, robot trajectory generation, multi-robot coordination for collision avoidance, and cycle-time calcula-

tion. The contribution of this integration is that it enables considering these aspects simultaneously within one problem, in order to co-adapt the optimal solution to each aspect. The methodology is investigated through a case study with consideration to multi-robot systems for material handling within a multi-stage sheet metal press line. Results show that optimising trajectories significantly reduces the part deformations.

2. Problem Formulation

The presented problem includes optimising the trajectory for each robot operation and coordinating these trajectories in time to avoid collisions between the robots that operate simultaneously in the same workspace. Additionally, the required forces to hold the part, part deformations, stresses induced in the part, and the cycle-time are checked to evaluate the trajectories.

In the presented problem, R is the set of robots in the system under consideration, and J is the set of joints of a robot. At time t, each Joint $j \in J$ of Robot $r \in R$ has a specific position $q_j^r(t)$, velocity $\dot{q}_j^r(t)$ and acceleration $\ddot{q}_j^r(t)$. The positions of the joints q_J^r determine robot pose and consequently, the end-effector's position vector $\{\mathbf{p}_E^r\}$ and orientation rotation matrix $\{\mathbf{R}_E^r\}$. In the operational space, the end-effector's linear velocity and acceleration will be referred to as $\mathbf{v}_E^r$ and $\mathbf{a}_E^r$, and the angular velocity and acceleration as ω_E^r and α_E^r respectively.

The path (specified by $\{\mathbf{p}_E^r\}$ and $\{\mathbf{R}_E^r\}$) that the end-effector follows through the workspace to move between the pick and place location is considered to be predefined for each material handling operation. These will be referred to as *end-effector paths*. Furthermore, the robot joint positions (q_j^r) for the sequence of robot poses to make the mounted end-effector follow its path are also considered as given. The sequence of joint positions for the robot poses will be referred to as *robot paths*. Finally, it is also assumed that each material handling operation is assigned to a specific robot and that the sequence of operations is predefined.

2.1. Problem Variables

The term *trajectory* is used in this paper to refer to the timing function for the movements of the robot (i.e. velocity and accelerations) along its predefined path. The variables that determine the trajectory are thus the robot joint velocities ($\dot{q}_j^r$) and accelerations ($\ddot{q}_j^r$). Hence, these are thus the variables of the trajectory optimisation problem. Additionally, the waiting-times (Δt^r) variables for the multi-robot coordination, i.e. the relative timing between the robot operations to avoid collisions when the robots that operate simultaneously in the same workspace also needs tuning when solving trajectory optimisation problem.

2.2. Problem's Objective

The objective of the trajectory optimisation problem is to minimise the part deformations during handling since, as elaborated earlier, reducing elastic deformations of the handled part decreases the risk of affecting its dimensional quality. The objective function for the problem formulation is written as follows

$$\min \sum_{r \in R} \Big(\max_{t \in [t_{pick},\, t_{place}]} (u_{max}^r(t)) \Big) \tag{1}$$

where $u_{max}^r(t)$ is the maximum deformation of the part handled by Robot r at time t. For the example of the deformed compliant sheet metal part shown in Figure 1, the maximum deformation (u_{max}^r) is the deformation of the part's boundaries in the x-direction. The dynamic deformations of the part during handling need to be known in order to determine the maximum deformation at time t. This can be calculated based on FEA transient response analysis with the force on the part during handling as input [17].

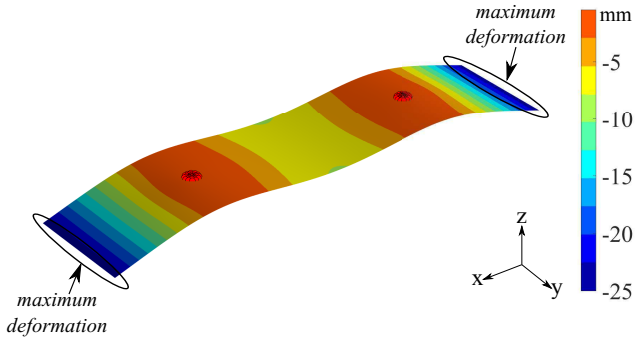

Figure 1: Example of maximum deformation of a handled part, i.e. compliant sheet metal plate (red dots indicate the vacuum-cups)

For material handling operations, the force that causes the part to deform is typically proportional to the combination of the gravitational acceleration and the end-effector's orientation, velocity and acceleration (i.e. drag and inertia force). The latter is, in turn, determined by the robot pose and thus, its joints' positions, velocities and accelerations. The maximum part deformation is formulated as follows

$$u_{max}^r(t) = f_1(q_J^r(t), \dot{q}_J^r(t), \ddot{q}_J^r(t)) \tag{2}$$

where function f_1 calculates the maximum deformation of the part resulting from the joint position, velocity and acceleration of Robot r at time t (implicitly considering the mass and inertia of the handled part).

2.3. Problem Constraints

The end-effectors can be equipped with vacuum-cups, magnetic-cups, fingers, or shovels to grip/hold a part. In order to securely pick place the part, the robot should be stationary during picking and placing; in other words its velocity should be zero. The following two constraints are included in the problem formulation to ensure this

$$\begin{aligned} \dot{q}_j^r(t_{pick}) &= 0 \\ \dot{q}_j^r(t_{place}) &= 0 \end{aligned} \tag{3}$$

where $\dot{q}_j^r(t_{pick})$ and $\dot{q}_j^r(t_{place})$ are the velocity of Joint j, respectively during pick and place of the part by Robot r, and t_{pick}

and t_{place} are respectively the time when the robot picks up and places the part.

The robots' end-effectors that hold the parts during handling have a specific maximum holding force. To prevent that a part is dropped during handling, it is necessary to ensure that the required force to hold the part never exceeds this maximum holding force. Similar as in (2) for the deformations, the force to hold the part is typically a combination of the acceleration induced inertia and drag forces, and is thus proportional to the robot joints' position (q^r_J), velocity ($\dot{q}^r_J$) and acceleration ($\ddot{q}^r_J$). Therefore, the problem formulation includes the following constraint

$$F^r(t) = g_1(q^r_J(t), \dot{q}^r_J(t), \ddot{q}^r_J(t)) \leq F^r_{hold} \tag{4}$$

where g_1 calculates the required force to hold the part $F^r(t)$ based on the robot joints' position, velocity and acceleration, and F^r_{hold} is the maximum holding force of the end-effector of Robot r. This constraint obviously only applies during the time-interval from t_{pick} until t_{place}, when a part is handled. The contact forces between the end-effector and the part (e.g. involving the suction forces for astrictive vacuum-cup end-effectors) are implicitly considered in equation g_1, as well as the part's mass and inertia.

In order to maintain the part's dimensional quality, plastic deformations during handling need to be avoided since these would introduce shape variations. Having to scrap damaged parts is very costly and has a large environmental impact [18]. The proposed objective function in (1) minimises the part deformations during handling, however, it does not guarantee that plastic deformations will not occur during any of the considered material handling motions. The problem formulation therefore includes a constraint to prevent plastic part's deformations by ensuring that the maximum induced stress in the part never exceeds the yield stress of the material. The yield stress is the stress at which a material starts to deform plastically and will not return to its original shape when the force is removed. The induced stress is proportional with the force on the part during handling. Similar to (4), this is formulated as follows

$$\sigma^r_{i,max}(t) = g_2(q^r_J(t), \dot{q}^r_J(t), \ddot{q}^r_J(t)) \leq \sigma^r_y \tag{5}$$

where g_2 is the function that gives the maximum induced stress $\sigma^r_{i,max}$ in the part resulting from the deformation that is caused by the forces due to the robot joints' position, velocity and acceleration at time t, and σ^r_y is the yield stress of the material of the handled part by Robot r (implicitly considering the part's mass and inertia). This obviously only applies during the time-interval from t_{pick} until t_{place}, when a part is handled.

The productivity is obviously also an important criterion for material handling in manufacturing systems. For this work, it is assumed that there is a certain degree of productivity that needs to be met, which is expressed as a predefined cycle-time. Hence, it is necessary to check that the system's cycle-time is equal to a predefined cycle-time in order to guarantee a certain productivity. The cycle-time of a multi-robot system depends on the trajectories, but is eventually determined by the robot coordination for these trajectories. This is expressed as follows for the problem formulation

$$Z = g_3(q^r_J(t), \forall t \in [t_{start}, t_{end}], \forall r \in R) = Z_{pre} \tag{6}$$

where Z is the cycle-time with the optimised trajectories, and Z_{pre} is the predefined cycle-time, g_3 is the collision-free multi-robot coordination function for the trajectories of the robots in the shared workspace of the robots in set R, and $q^r_J(t)$ represents the pose of Robot r in time $\forall t \in [t_{start}, t_{end}]$ for the J joints' positions of each Robot $r \in R$. In this work, the collision-free multi-robot coordination is not solely realised by tuning the trajectories, but the system also uses an initial waiting-time (Δt^r) to make a robot wait to start its operation so that it will not collide with the robot of the previous operation in the shared workspace [8]. The proposed optimisation model directly calculates the minimal initial waiting-times for collision-free multi-robot coordination based on the robots' trajectories.

3. Proposed Optimisation Model

This section describes how the proposed optimisation model represents the problem formulated in Section 2, and how it is parametrised. In order to solve the formulated problem by optimising the multi-robot trajectories, it is modelled as a non-linear programming (NLP) optimisation problem based on the earlier work by Glorieux et al. [8]. The predefined robot paths are first discretised into n segments, which gives the positions $q^r_{j,i}$ for each Joint $j \in J$ of each Robot $r \in R$, for each Segment $i \in N = \{1, \ldots, n\}$. The end-effector paths are correspondingly discretised into $\mathbf{p}^r_{E,i}$ and $\mathbf{R}^r_{E,i}$ accordingly for each Segment $i \in N$.

3.1. Optimisation Model Variables

A series of time variables t^r_i are introduced for each Robot r that specify the duration for each Segment i. By tuning these segment duration time variables (t^r_i), the angular velocity ($\dot{q}^r_{j,i}$) and angular acceleration ($\ddot{q}^r_{j,i}$) of each Joint $j \in J$ of Robot r are being optimised, for each Segment i, and thereby its trajectory. In this way, the optimisation variables for the considered problem are only the segment duration-times (t^r_i). The trajectories are approximated in the NLP model as having piece-wise constant acceleration that only changes at the end of each segment. These relationships are approximated in the NLP model using the following equations

$$\begin{aligned} \dot{q}^r_{j,i+1} &= \dot{q}^r_{j,i} + \ddot{q}^r_{j,i} \cdot t^r_i \\ q^r_{j,i+1} &= q^r_{j,i} + \dot{q}^r_{j,i} \cdot t^r_i + \ddot{q}^r_{j,i} \cdot (t^r_i)^2/2 \end{aligned} \tag{7}$$

where $\dot{q}^r_{j,i}$ and $\ddot{q}^r_{j,i}$ are respectively the velocity and acceleration of Joint j of Robot r during Segment i. The end-effector velocities ($\mathbf{v}^r_{E,i}$ and $\omega^r_{E,i}$) and accelerations ($\mathbf{a}^r_{E,i}$ and $\alpha^r_{E,i}$) for each Segment i are then derived based on the predefined end-effector path ($\mathbf{p}^r_{E,i}$ and $\mathbf{R}^r_{E,i}$) and the segment duration-times (t^r_i).

At the start and end of the operation, the robot is stationary. It thus needs to be ensured that the robot joints' velocity and acceleration are zero at the start and end of the operation. This is

realised by implementing the following constraints in the NLP model

$$\begin{aligned} \dot{q}^r_{j,1} &= 0; \quad \dot{q}^r_{j,n} = 0; \\ \ddot{q}^r_{j,1} &= 0; \quad \ddot{q}^r_{j,n} = 0; \end{aligned} \tag{8}$$

where $i = 1$ refers to the beginning of the trajectory and $i = n$ to the end. Similar constraints are used to ensure that the robot stands still at the positions for picking or placing the part

$$\dot{q}^r_{j,pick} = 0; \quad \dot{q}^r_{j,place} = 0; \tag{9}$$

where $\dot{q}^r_{j,pick}$ and $\dot{q}^r_{j,place}$ are the velocity of Joint j respectively for the pick and place segment of the operation performed by Robot r. This shows how the equation in (3) are implemented in the proposed NLP model.

The following boundary conditions are implemented in the NLP model to specify the allowed range for the values of the optimisation variables (i.e. for segment duration times) and indirectly also the robot joint velocities and accelerations

$$\begin{aligned} t_{min} &\leq t^r_i \leq t_{max} \\ \dot{q}^r_{j,min} &\leq \dot{q}^r_{j,i} \leq \dot{q}^r_{j,max} \\ \ddot{q}^r_{j,min} &\leq \ddot{q}^r_{j,i} \leq \ddot{q}^r_{j,max} \end{aligned} \tag{10}$$

where t_{min} and t_{max} are respectively the minimum and maximum duration time (see Section 6.1 for further details), and $\dot{q}^r_{j,min}, \dot{q}^r_{j,max}$ and $\ddot{q}^r_{j,min}, \ddot{q}^r_{j,max}$ are the lower and upper limits for respectively the velocity and acceleration of the robot joints.

The robot movements also need to be reasonably smooth in order to avoid strong vibrations and stresses in the robot's structure and components, which would increase the wear rate [19]. Smooth trajectories have good continuity in terms of the joints' accelerations. To achieve this, the jerk (i.e. the derivative of the acceleration) is limited by implementing the following constraint that specifies a boundary on the jerk to control the smoothness of the trajectory

$$\frac{|\ddot{q}^r_{j,i+1} - \ddot{q}^r_{j,i}|}{t^r_i} \leq \dddot{q}^r_{j,max} \tag{11}$$

where $\dddot{q}^r_{j,max}$ is the maximum allowed jerk for the Joint j. The optimisation variable t^r_i determines thus not only the joints velocity and acceleration but also the jerk during Segment i. When the maximum allowed jerk value $\dddot{q}^r_{j,max}$ is unknown, a good approximation can be obtained by examining the maximum jerk of trajectory generated (at high/maximum robot velocity) by the robot supplier's controller for the specific predefined robot path [8].

3.2. Force Calculation

Based on equations (4)-(5), it is required to estimate the force on the part during handling in order to calculate the objective function. It is assumed in this work that the force (F^r_i) on the part is a combination of the acceleration-induced inertia force and the drag force. These are proportional with respectively the robot joints' velocity ($\dot{q}^r_J$) and acceleration ($\ddot{q}^r_J$), and the gravitational acceleration. However, the force can be expressed directly in terms of the end-effector (linear) velocity ($\mathbf{v}^r_{E,i}$) and accelerations ($\mathbf{a}^r_{E,i}$ and $\alpha^r_{E,i}$), since the proposed NLP model directly derives these based on the optimisation variables (t^r_i). Furthermore, the orientation of the end-effector $\mathbf{R}^r_{E,i}$ needs to be taken into account for calculating the drag force. Consequently, the equation to calculate the force on the part in the model can be written as follows

$$F^r_i = f_{FORCE}(\mathbf{R}^r_{E,i}, \mathbf{v}^r_{E,i}, \mathbf{a}^r_{E,i}, \alpha^r_{E,i}) \tag{12}$$

where f_{FORCE} estimates the force on the part F^r_i based on the end-effector's orientation ($\mathbf{R}^r_{E,i}$), linear velocity ($\mathbf{v}^r_{E,i}$), linear and angular accelerations ($\mathbf{a}^r_{E,i}$ and $\alpha^r_{E,i}$). The function f_{FORCE} can be split into two separate terms, one for the inertia force and the other for the drag force, so that

$$F^r_i = F^r_{inertia,i} + F^r_{drag,i} \tag{13}$$

where the inertia force $F^r_{inertia,i}$ can be expressed as follows

$$F^r_{inertia,i} = m^r_p \cdot (\mathbf{a}^r_{E,i} + g) + I^r_p \cdot \alpha^r_{E,i} \tag{14}$$

where g is the gravitational acceleration, m^r_p is the mass, and I^r_p is the inertia of the handled object. The drag force $F^r_{drag,i}$ can be expressed as follows

$$F^r_{drag,i} = \frac{1}{2} \cdot \rho_a \cdot (\mathbf{v}^r_{E,i})^2 \cdot C^r_d(\mathbf{R}^r_{E,i}) \cdot A^r_{p,d}(\mathbf{R}^r_{E,i}) \tag{15}$$

where ρ_a is the density of air, $C^r_d(\mathbf{R}^r_{E,i})$ is the drag coefficient and $A^r_{p,d}(\mathbf{R}^r_{E,i})$ the drag area of the handled part for the specific orientation $\mathbf{R}^r_{E,i}$ of the end-effector.

3.3. Objective Function Modelling

The objective function in (1) minimises the dynamic part deformations during handling. Finite Element Analysis (FEA) is typically used to model the dynamic deformations based on the transient response analysis resulting from the dynamic forces on a part during the handling motion. However, directly integrating FEA and the transient response analysis for estimating the dynamic part deformations in a NLP model would result in a very time-expensive model. Hence, an alternative approach is proposed in this paper to effectively implement an objective function that minimises the deformations of the handled part in order to protect its dimensional quality.

As a first simplification, it is proposed in this work to model the steady-state part deformation resulting from the force on the part during each individual path segment instead of modelling the dynamic part deformations to remove the need to calculate the transient response analysis. To compensate for this simplification, it is proposed to not consider the maximum steady-state deformation across the trajectory segments but instead the sum of the squared steady-state part deformations during each individual segment for the objective function in this work. This gives the following deformation minimisation objective function

$$\min \sum_{r \in R} \sum_{i \in H} (u^r_{i,max})^2 \tag{16}$$

where $u^r_{i,max}$ is the maximum deformation of the part held by Robot r during Segment $i \in H$, and set $H \subset N$ is the subset with

the indices for the segments during which the robot holds a part. For the example of pick and place material handling operations, the indices of the segments in between the pick ($i = pick$) and place ($i = place$) segments are in the set H since the robot then handles the part. Based on (2), the force on the part during handling determines the maximum deformation of the part, and can therefore be written as the following function

$$u^r_{i,max} = f_{DEF}(F^r_i),\ \forall i \in H \tag{17}$$

where f_{DEF} is a function that gives the steady-state part deformation for the force F^r_i on the part during individual Segment i. The force F^r_i is obtained using (12).

Secondly, in order to remove the need to integrate the FEA in the NLP model, a Response Surface Model (RSM) is used to represent the relationship between the force on the part and the resulting deformations. The RSM is constructed in advance based on regression modelling of sampled FEA results. Integrating the constructed RSM in the NLP model is significantly more time-efficient compared to using FEA. This is integrated in the model as follows

$$u^r_{i,max} = \mathrm{RSM}_u(F^r_i),\ \forall i \in H \tag{18}$$

where $\mathrm{RSM}_u(F^r_i)$ is a function that represents the RSM. In other words, RSM_u replaces the function f_{DEF} in (17).

To construct the RSM, a set of samples is generated first and each sample has a different value for the input parameter, i.e. the force on the part. Depending on the application range for the force on the part, the samples can be obtained for example by random sampling (done in this work) or by uniform sampling. A physics-driven model with a FEA-based kernel is solved for each sample to calculate the corresponding output value for the maximum part deformation [20]. FEA requires a representation of the part, how it is held by the end-effector's gripper, and the forces that are acting on the part. For example, vacuum-cups which are commonly used on material handling end-effectors, can be represented for the FEA by a rigid point model [2] or a dexterous spring model [1]. The former is used in this work.

The RSM is constructed by performing a regression modelling of the samples. The selection of the regression technique can vary depending on the complexity and non-linearity of the problem. Non-linear polynomial fitting is used in this work, as proposed by Li and Ceglarek [4], and the accuracy is verified by performing a non-exhaustive leave-p-out cross validation.

3.4. Problem Model Constraints

a. Yield Stress Constraint

The yield stress constraint from (5) is necessary to avoid plastic deformation by ensuring that the induced stress in the handled part does not exceed the material's yield stress. The induced stress is, just as the deformation, proportional to the force on the part during handling, and can thus be written as follows

$$\sigma^r_{i,max} = f_\sigma(F^r_i) \leq \sigma^r_y,\ \forall i \in H \tag{19}$$

where $\sigma^r_{i,max}$ is the maximum stress in the part resulting for force F^r_i acting on the handled part. The maximum *von Mises* stress is used as indicator for comparing the induced stress in the part with the yield stress. As it is an equivalent stress, the *von Mises* stress does not relate linearly to the force on the part. FEA is typically used to estimate the *von Mises* stress induced in the deformed part. Therefore, a RSM is used instead for representing the relationship between the force on the part and the induced stress in the proposed NLP model, for the same motivation as in case of the deformations. Only the maximum stress in the part is relevant for the yield stress constraint.

The used RSM is constructed in the same way as described in Section 3.3 for the part deformations. This results in the following function

$$\sigma^r_{i,max} = \mathrm{RSM}_\sigma(F^r_i) \tag{20}$$

where $\mathrm{RSM}_\sigma(F^r_i)$ is a function that represents the RSM to estimate the induced stress and the force F^r_i on the part is obtained using (12).

b. Holding Force Constraint

The holding force constraint (4) verifies that the part is not dropped from the end-effector during handling. This is done by ensuring that required force to hold the part never exceeds the maximum holding force of the end-effector. The implementation of the constraint can then be written as follows

$$F^r_i \leq F^r_{hold},\ \forall i \in H \tag{21}$$

where F^r_{hold} is the maximum holding force of the end-effector that holds the part handled by Robot r. It is assumed that the required force to hold the part is equal to the force on the part and can thus be calculated using (12).

When the end-effector layout is asymmetric to the part's centre of gravity, there is an additional momentum force, which possible reduces the maximum holding force of astrictive end-effectors. The maximum holding force of the end-effector is therefore thus dependent on its design. Tuleja and Sidlovská [21] and Mantriota and Messina [22] propose calculation methodologies for the maximum holding force of respectively tangential loads and symmetric/asymmetric layouts around the part's centre of gravity for end-effector designs with vacuum-cups. The maximum holding force of the end-effector is calculated based on these works.

c. Cycle-Time Constraint

As mentioned earlier, it is assumed there is a predefined required productivity for the considered material handling system. As formulated with (6), it is necessary to check that the cycle-time with the optimised trajectories agrees with the predefined cycle-time for the required productivity. This is implemented in the proposed NLP model by including the following constraint

$$Z \leq Z_{pre} \tag{22}$$

where Z_{pre} is the predefined cycle-time and Z is the cycle-time with the optimised trajectories. The cycle-time is on the one hand determined the duration of the robot trajectories, and on

the other hand by the multi-robot coordination to avoid collisions between the robots. In this work, the multi-robot coordination is not only achieved by tuning the timing function for the robot trajectories but also when necessary, the start of a robot operation is delayed to ensure that its trajectory in the workspace will be available, so that it will not collide with the robot of the previous operation [8]. In other words, the robots are coordinated by initial waiting-times, relative to the start of the previous operation. Let Δt^r be the duration of the initial waiting-time for the operation performed by Robot r. Then, Robot r starts Δt^r *seconds* after the start of Robot $r-1$. The initial waiting-times (Δt^r) are furthermore also adjusted concerning the availability of the robot, since it has to wait until the operation for the previous cycle is completed before starting the next one. When the initial waiting-times have been tuned, the cycle-time of the system can be expressed as follows

$$Z = \sum_{r \in R} (\Delta t^r) \tag{23}$$

equal to the sum of all robots' initial waiting-times.

This work adopts a *decoupled approach* for the multi-robot coordination, which uses priorities to enable performing the trajectory optimisation independently for each robot [23]. Decoupled approaches for multi-robot motion planning problems are more efficient compared to *centralised approaches*, although they typically sacrifice in completeness [23]. The multi-robot coordination method used in the proposed NLP model is adopted from the work by Glorieux et al. [8], which thus allows that the trajectories are optimised independently while the model directly updates the minimal initial waiting-times (Δt^r) required to avoid collisions. Furthermore, based on these waiting-times and the duration of the robot trajectories, it also directly determines the resulting cycle-time based on (23). In order to implement the multi-robot coordination in the proposed NLP model, the potential collisions between the robots along the predefined trajectory need to be mapped into the spatial representation based on relative robot position [8]. This can usually be done very efficiently by using a fast 3D collision detection simulation, and simplified CAD models that approximate the geometry of the robots, end-effectors and handled parts. A detailed description of the multi-robot coordination method used in the proposed NLP model is given by Glorieux et al. [8]. The multi-robot coordination method thereby enables the proposed NLP model to verify the constraint from (22) in order to guarantee a predefined productivity, and thereby integrates (6) .

3.5. Optimal Solution Post-Processing

The output of the proposed NLP model is a list of optimised duration-times t_i^r for each Segment i of each Robot r and the corresponding initial waiting-times Δt^r for the multi-robot coordination. Post-processing is necessary to obtain the corresponding optimised trajectories. Interpolation can be used to get the robot positions for *isochronal* time-steps to reformulate the optimised trajectories. Isochronal time-steps means that they have an equal time-duration. A trajectory in this format is suitable as it can typically be programmed and uploaded to a robot or an industrial material handling device.

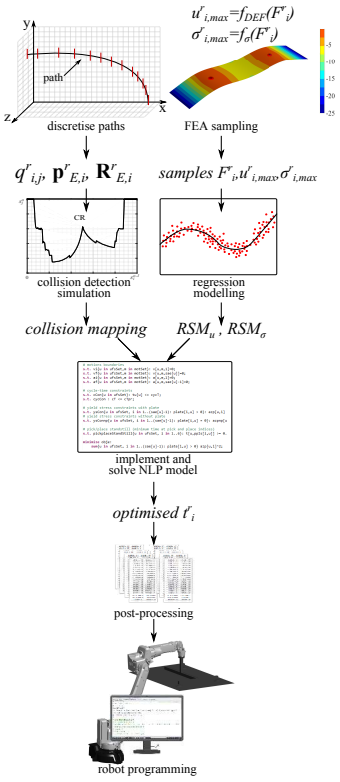

Figure 2: Flowchart of the proposed optimisation methodology

4. Optimisation Procedure

This section describes the application of the proposed methodology on an industrial multi-robot system for material handling of compliant parts. Figure 2 shows the flowchart of the procedure. It starts with obtaining the predefined paths for each Robot r. These are then discretised to obtain the positions of the robot joints for all n segments. The next step is to generate the mapping of the potential collisions between every robot-pair that operates simultaneously in a shared workspace. This is done directly using (simplified) CAD models of the robots' structure, end-effectors, and handled parts. A 3D collision detection simulation with the discretised predefined paths and CAD models of the robots/end-effectors/parts needs to be performed, and the registered collisions are then included in the relative robot-position based mapping.

It is also necessary to generate data samples concerning the deformation and induced stresses resulting from forces with different magnitudes on the handled part. This is done using FEA. When sufficient samples have been generated, these are used for the regression modelling in order to generate the two RSMs, i.e. one for modelling the part deformations (18), and the other for the induced stresses (20).

The next step is to implement the proposed NLP model, which includes determining the limits of the optimisation variables, i.e. for the time, velocity, acceleration and jerk for the robot joints, in order to implement constraints (10) and (11). In case where these limits are not directly available for the robots, these can be approximated based on the limits of trajectories

for the operations generated by the controller provided by the robot's supplier. The predefined cycle-time needs to be determined to implement constraint (22). The mapping of the collision between the robots that operate in the shared workspace are used to implement constraint (23) for the multi-robot coordination. The objective function (16) is then also implemented in the NLP model.

When the implementation of the NLP model is complete, the next step is to optimise the trajectories accordingly. This is done by using a non-linear solver, for example, the Knitro non-linear solver [24] that is used in this work. Note that there typically are several options of the solver concerned with, for example, algorithm, termination conditions, feasibility tolerances, derivatives, etc. that need to be specified.

The relevant output of the proposed NLP model are the optimised segment duration-times (t_i^r) for each Robot r, and the initial waiting-times (Δt^r) for the multi-robot coordination. Post-processing is necessary to convert the optimised segment duration-times into a trajectory that can be specified in a suitable format to be programmed and uploaded to the robot.

The final step is to implement the optimised trajectories with the interpolated timing-function in the robot program and integrate the initial waiting-times (Δt^r). Note that special rules might be required for the first and last cycles of the multi-robot system, as the trajectories and multi-robot coordination are optimised for the complete production system in full operation.

5. Case Study

This section describes the application of the proposed trajectory optimisation methodology with consideration to material handling in a multi-stage press line for stamping sheet metal parts. The motion planning of the material handling in press line is challenging due to the close interaction between the presses and robots, while it is also a critical issue for the industry [25].

The case study considers the material handling of the first press in the line, and it thus consists of two robots and a press, as shown in Figure 3. Robot 1 picks up the plate from Table 1 and loads it into the press, while Robot 2 unloads the plate after it is stamped by the press and places it onto Table 2. The robots are 2D-belt Binar UniFeeder robots for material handling [26]. The end-effectors use vacuum-cups to hold the sheet metal plates.

For the robot coordination, the press is considered as a special type of robot as it also forms a moving obstacle in the shared workspace. This special type of robot has only a single degree-of-freedom, and there is a predefined path and trajectory for its operation. This means that only its initial waiting-time needs to be tuned by the optimisation.

The sequence of robot and press operations for the case study is predefined. It starts with Robot 1 loading a blank plate into the press, followed by the press performing the stamping operation, then Robot 2 unloads the stamped plate, and is thereafter repeated for the next cycle. These three operations need to be coordinated since these take place in the same workspace.

The press considered in this case study corresponds to the first press in the multi-stage press line. This is considered since it specifically is an interesting case as the material handling for the first press in a line is typically the most critical and therefore, often a bottleneck for multi-stage press lines [2]. The plates that are loaded into that press usually are blank sheet metal plates, i.e. flat plates. These are relatively more compliant because, in the next stages of the press line, the plates become stiffer and thus, less compliant when they are stamped and trimmed.

The case study considers the specific setup of the multi-stage press line that is dedicated for the production of an inner side panel of the floor frame for a car body. The handled part is the blank sheet metal plate with dimensions 1975x460x1.4 *mm* and the material is steel DP800.

6. Implementation

This section presents the details of the implementation of the proposed NLP model for the case study of the sheet metal press line. The press is seen as a special case of a robot which has one degree-of-freedom and its trajectory is predefined and cannot be modified. Together with the two material handling robots, there are in total three robots in the system ($R = \{1, 2, 3\}$). The 2D-belt material handling robots have two joints ($J = \{1, 2\}$), and the special robot that represents the press has one joint.

The robot paths for both material handling robots are identical, and is shown in Figure 4. For Robot 1, the press is on the right side at the place location, and for Robot 2, the press is on the left side at the pick location.

The proposed NLP model is implemented using the software package AMPL (A Modelling Language for Mathematical Programming) [27] and it is solved using the Knitro non-linear solver [24].

6.1. Optimisation Variables

The lower and upper limit of the boundary condition in (10) for the segment duration times (t_i^r) need to be in line with the discretisation of the predefined path for the operation. The discretisation of the paths is therefore based on isochronous sampling (i.e. 0.005 seconds) of a "reference" trajectory that is generated by a computer model of the robot's controller (at maximum speed). Determining the boundary limits for the t_i^r optimisation variables is then more straightforward. For the case study in this work, the boundary limits of t_i^r are then $t_{min}^r = 0.001$ seconds and $t_{max}^r = 0.050$ seconds.

The lower and upper limits of the boundary conditions of (10) for velocity, and acceleration optimisation variables are not known explicitly for the 2D-belt Binar UniFeeder robot. These are therefore estimated based on the minimum/maximum velocity and acceleration of the controller's "reference" trajectory.

Similarly, the value for the maximum allowed jerk $\dddot{q}_{max}^r$ for robot joints in the smoothness constraint (11) is also determined based on the controller's "reference" trajectory. The used value for $\dddot{q}_{max}^r$ in the proposed NLP model is the same as the maximum jerk of the controller's "reference" trajectory.

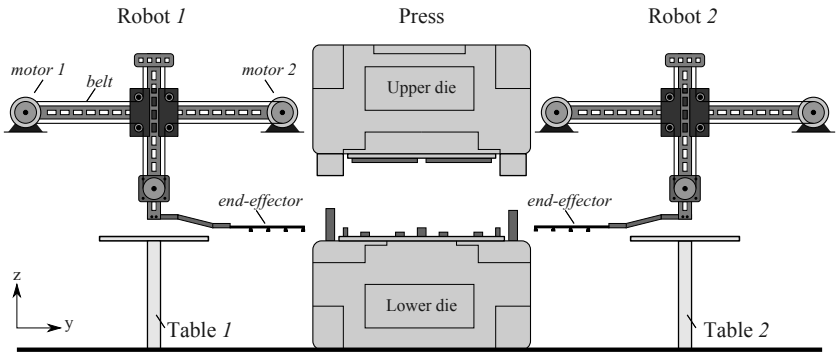

Figure 3: Illustration of the single press with two press tending robots (loading and unloading) of the considered case study

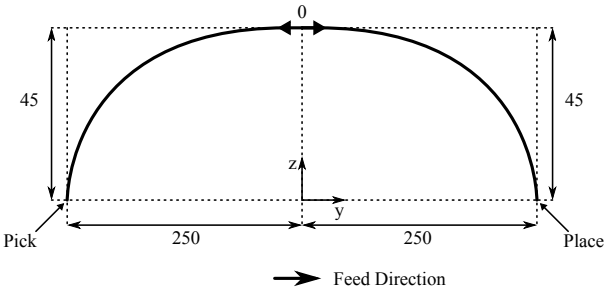

Figure 4: Illustration of the robot path for the material handling in the press line

6.2. Force

In the case study, the orientation of the end-effectors that are mounted on the 2D-belt press tending robots does not change along the paths. Hence, the angular acceleration and the resulting inertia force are therefore always zero and these can thus be ignored. Furthermore, as the handled parts in this case study are blank sheet metal plates, the forces in vertical direction will have a larger influence on the part deformation than the forces in horizontal direction. The force calculation in the proposed NLP model therefore focusses only on the forces in vertical direction for this case study. The equation to calculate the acceleration-induced inertia force $F^r_{inertia,i}$ in (14) can thus be reformulated as follows

$$F^r_{inertia,i} = m^r_p \cdot (g + \mathbf{a}^r_{E,i,z}) \tag{24}$$

where $\mathbf{a}^r_{E,i,z}$ is the acceleration in z-direction (vertical) of the end-effector that is holding the part handled by Robot r during segment i of the path, g is the gravitational acceleration, and m^r_p is the mass of the part. The equation to calculate the drag force $F^r_{drag,i}$ on the part can be reformulated as follows

$$F^r_{drag,i} = \frac{1}{2} \cdot \rho_a \cdot (\mathbf{v}^r_{E,i,z})^2 \cdot C^r_d \cdot A^r_{xy} \tag{25}$$

where ρ_a is the density of air, $\mathbf{v}^r_{E,i,z}$ is the velocity in z-direction (vertical) of the end-effector of Robot r during Segment i of the path, C^r_d is the drag coefficient for the geometry of the part, and A^r_{xy} is the area in xy-plane of the part. For example, a flat plate perpendicular to the airflow has a drag coefficient C^r_d is equal to 2.0.

6.3. Objective Function

The *Variation Response Method (VRM)* [28], a physics-driven modeller with FEA-based kernel, is used in this work to evaluate the samples for constructing the deformation response surface model RSM_u in (18) because of its advanced capabilities to parametrise key aspects including the force, part's compliance, end-effector, and vacuum-cups [29, 30]. The vacuum-cups are modelled as a set of rigid points in a circular pattern. It is assumed that the positions of the vacuum-cups relative to the plate are fixed during handling and are identical for each cycle.

The regression modelling to construct RSM_u is based on 100 samples, which are generated by random sampling. It was found that this number of samples is sufficient to construct an accurate 3rd order polynomial regression model for the RSM_u, i.e. *root-mean-square error* is less than 1 *mm*.

6.4. Problem Constraints

a. Yield Stress Constraint

The samples for constructing the induced stress response surface model RSM_σ for (20) are also generated using the physics-driven modeller with FEA-based kernel VRM. Again, 100 random samples are generated for the regression modelling, which results in an accurate 3rd order polynomial regression model for the RSM_σ, i.e. *root-mean-square error* is less than 2.50 *MPa*.

b. Holding Force Constraint

Two circular vacuum-cups with a diameter of 54 *mm* are mounted on the end-effectors in order to hold the handled sheet metal plate. The maximum holding force of each vacuum-cup is 72 *Newton* in the normal direction. The location of the vacuum-cups on the sheet metal part is symmetric around the centre-of-gravity of the plate, and each at 493.75 *mm* to the plate's sides in longitudinal direction. In total, the maximum holding force of the end-effector is thus $F^r_{hold} = 144$ *Newton*.

c. Cycle-Time Constraint

Three scenarios where two robots (or press) operate simultaneously in a shared workspace need to be considered during the multi-robot coordination for the material handling system in the case study, which is illustrated in Figure 3, in order to avoid collisions. These three scenarios are:

1. stamping: collision between the upper die of the press and the empty end-effector of Robot 1,
2. unloading: collision between the upper die of the press and the empty end-effector of Robot 2,
3. loading: collision between the plate held by the end-effector of Robot 1 and the plate held by the end-effector of Robot 2.

For multi-robot coordination according the method proposed by Glorieux et al. [8], collision detection simulations are performed in advance using the PQP library [31] for its fast collision detection calculations between 3D CAD models. These CAD models, i.e. of the geometry of the robots and press, are directly taken from the considered real-world press-line.

6.5. Optimal Solution Post-Processing

The post-processing interpolates the found optimal solution so that it is reformulated as the robots' position for isochronal time-steps of 0.005 seconds. In this format, the optimised trajectories are implemented in the robot program.

For the experimental tests in this work, the robot program with the optimised trajectories are then uploaded to a 2D-belt Binar Unifeeder robot in a laboratory setup. This allows testing different trajectories for verifying and validate the proposed NLP model, and to compare the optimised trajectories by the robot controller's trajectories.

7. Validation and Evaluation

This section presents the performed tests with the case study to validate and evaluate the proposed optimisation methodology. Several tests are done to optimise and evaluate trajectories on a robot. The goal is to evaluate the optimised trajectories with reference trajectories that are generated by the robot controller provided by the supplier. The robot motion is recorded when the trajectories are performed on the robot and the recorded motion data is then analysed using the FEA in order to compare part deformations that occur with the tested trajectories.

7.1. Tests

Two sets of trajectories for the robots in the case study are generated for the same cycle-time. The first ones are reference trajectories that are generated according to the robot controller provided by the supplier. They are obtained using an advanced model of 2D-belt Binar Unifeeder robot's controller [32]. The second set of trajectories are optimised with the proposed methodology for the same cycle-time as calculated for the reference trajectories.

In the tests to validate the proposed methodology, both sets of trajectories are executed on a 2D-belt Binar Unifeeder robot. During this, the robot joints' motions are recorded to obtain a measurement for these trajectories. These measurements are analysed and compared to the modelled trajectories. The main relevant aspect of a trajectory for minimising part deformations is the force in the vertical direction on the part, and the resulting part deformations. The analysis of the trajectories therefore includes calculating the profile of the resulting force on the part, and the corresponding part deformations. It should be noted that now the dynamic part deformations are calculated using FEA and by performing the transient response analysis, in order to also validate the approximation in the proposed NLP model based on RSM_u. The reference and optimised trajectories are compared with each other to demonstratively evaluate the deformation minimisation with the proposed methodology.

Table 2: Comparison of maximum vertical force and dynamic part deformations for the measured reference and optimised trajectories

	F^r_{max} [N]		Δ	u^r_{max} [mm]		Δ
	org	*opt*	[%]	*org*	*opt*	[%]
Robot 1	-145.7	126.5	-13	-30.2	-26.9	-12
Robot 2	-145.0	125.4	-14	-29.6	-26.1	-13

7.2. Results

The reference trajectories generated by the robot controller have a duration of 1.50 *seconds*. However, due to initial waiting-times for the multi-robot coordination for the reference trajectories to avoid collisions, the resulting cycle-time of the material handling system in the case study turned out to 1.70 *seconds*. The predefined cycle-time in (22) in the proposed NLP model was thus set to this values, i.e. Z_{pre} = 1.70 *seconds*.

The graphs with the modelled and measured position profiles of the two robot joints are shown for the reference trajectory in Figure 5a and 5b, and for the optimised trajectory in Figure 5c and 5d. It can be seen that in all four graphs, the measured position profile corresponds reasonably well with the modelled position profile. In fact, the difference in the robot's position between the modelled and measured trajectories is calculated to quantify the similarity. The maximum difference for the robot position is around 12 *mm* for the reference trajectories, and around 15 *mm* for the optimised trajectories. The calculated vertical force profiles along both the modelled and measured trajectories are shown in Figure 6a and 6b, respectively for the reference and optimised trajectory.

The comparisons of the force on the part with the reference and optimised trajectories are presented by the force profiles presented in Figure 7. The shaded areas indicate the sections of the trajectories during which a part is handled. Hence, these sections of the trajectories are relevant when comparing the part deformations. Table 2 shows the maximum vertical force (F^r_{max}) along the trajectory when handling a part, for the different tests. Furthermore, the results for the maximum dynamic part deformations (u^r_{max}) calculated by the FEA for the different measured profiles are also shown in Table 2.

7.3. Discussion

a. Validation

The first purpose of the performed tests and investigation is to validate the trajectories generated with the proposed optimi-

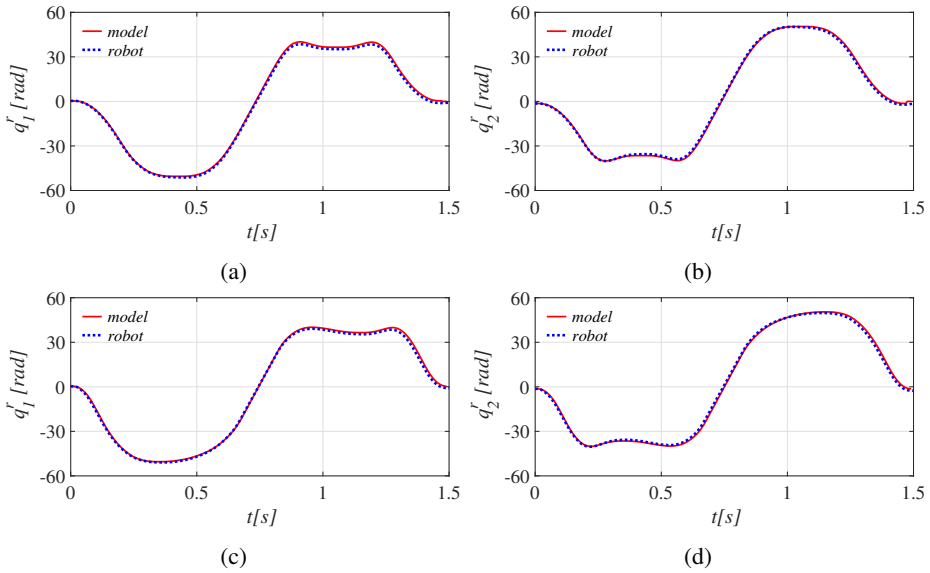

Figure 5: Comparison modelled *(model)* and measured *(robot)* joint motions, comparison of the controller's reference trajectories, (a) Joint 1 reference, (b) Joint 2 reference, (c) Joint 1 optimised, (d) Joint 2 optimised

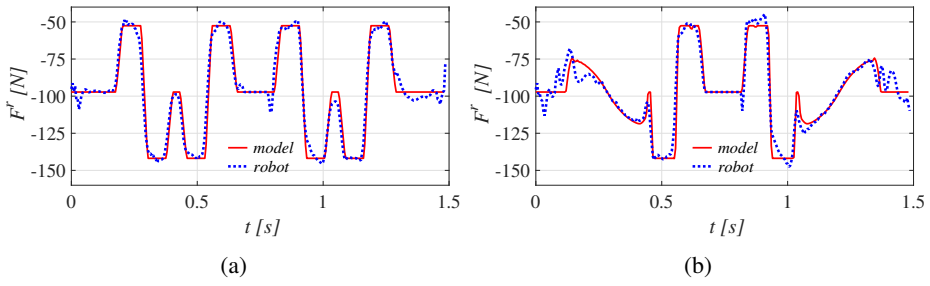

Figure 6: Comparison modelled *(model)* and measured *(robot)* profiles of the vertical force on the part for (a) reference and (b) optimised trajectory

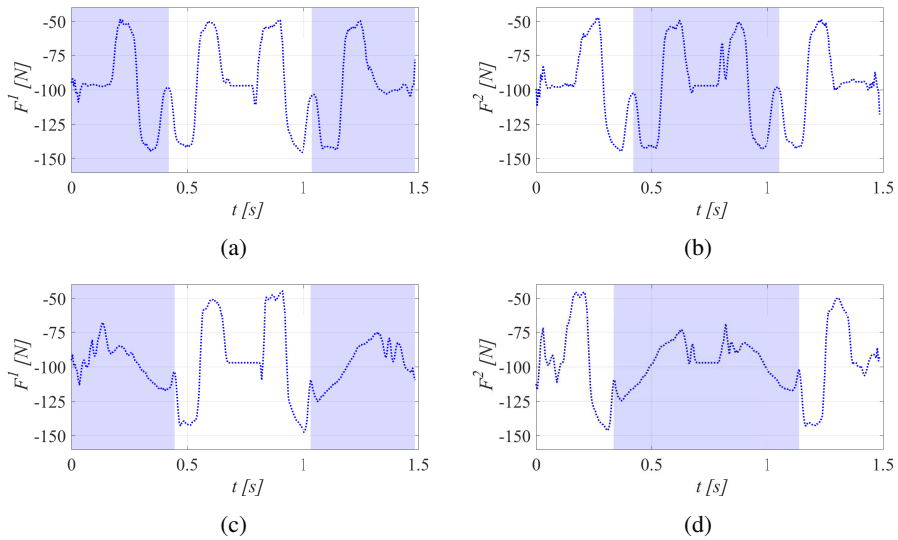

Figure 7: Profiles vertical force on the part, shaded areas indicate when the robot handles a part, for (a) Robot 1 reference, (b) Robot 2 reference, (c) Robot 1 optimised, (d) Robot 2 optimised trajectory

sation methodology. The accuracy of the modelled robot position for the optimised trajectories is important for the reliability of the proposed methodology. Specifically, it is relevant for the collision avoidance by the multi-robot coordination and the cycle-time calculation in (6). The trajectory validation results in Figure 5 show that the "model-to-measurement" correspondence for the robot position with the optimised trajectories is as good as with the reference trajectories. This indicates that the modelled optimised trajectories are equally reliable as the modelled reference trajectories. These results thus validate the trustworthiness of the modelling of the multi-robot trajectories in the proposed optimisation methodology.

It is also critical that the force calculation in (12) for the proposed methodology is reliable since it relevant for the estimating the maximum part deformations (18) on which the objective function is based, and also for constraints (20)-(21). Even if the difference in robot position is relative small, it is still necessary to check whether there are no significant differences in the force on the handled part. The results in Figure 6 concerning the force profiles of the modelled and measured trajectories show that there is a good correspondence between these two, for both the reference and optimised trajectories. Since there are no problematic difference in the force profiles, it can be stated that this validates the force calculation in the proposed optimisation methodology.

The final element for validating the modelling of the trajectories is to check if there is a significant difference in part deformations for the modelled and measured profiles. For the reference trajectory, the estimated maximum deformation is -29.2 *mm* for the modelled and -29.6 *mm* for the measured trajectory. Whereas, for the optimised trajectory, the estimated maximum deformation is -26.0 *mm* for the modelled and -26.1 *mm* for the measured trajectory. This shows that the maximum deformations for the modelled and measured trajectory corresponds equally well for the optimised trajectory as for the reference trajectory. It can thus be stated that the trajectory modelling by the proposed optimisation model is thus also reliable for estimating the part deformations.

b. Evaluation

The second purpose of the performed tests and investigation is to demonstratively evaluate the deformation minimisation with the proposed optimisation methodology for the considered case study. Figure 7 and Table 2 thus present the results for this. The force profiles in Figure 7 show how the optimisation methodology reduces the force for the trajectory segments when the robot handles the part. It can be seen that profiles of the optimised trajectories are significantly lower in the shaded areas, i.e. when a part is handled, for Robot 1 in Figure 7c and for Robot 2 in Figure 7d compared to force profiles with the reference trajectories in Figure 7a and 7b. On the other hand, the profiles have a similar shape when the robots are not handling a part. The results presented in Table 2 quantify the difference in force on the part between the reference and optimised trajectories. The results show that for both robots, the maximum vertical forces are significantly lower, i.e. around 13%, for the optimised trajectories compared to the reference trajectories.

The corresponding maximum part deformation for the force profiles of the reference and optimised trajectories are also presented in Table 2. There is indeed thus a significant difference in estimated part deformations during handling between the original and optimised trajectories. The magnitude of the part deformations is 12% smaller for Robot 1, and 13% smaller for Robot 2. The differences in maximum vertical force on the part for the original and optimised trajectories are similar in magnitude. Note that the cycle-time of the complete system remains the same. This demonstfrates a valuable reduction in part deformations with the optimised trajectories to enhance the certainty that the dimensional quality of the part is maintained.

c. Result Interpretation

This section provides a discussion on the interpretation and relevance of the obtained elastic deformation minimisation results by the trajectory optimisation. As mentioned earlier, the motivation for minimising elastic deformations is due to the relationship with nesting errors and part distortions occurring when dropping the part at the place location [1]Ṫhe magnitude of the remaining elastic deformation needs to be put into context regarding their effect on the dimensional quality of the handled part.

It is proposed in this work to group part deformations during handling in three different categories for the purpose ensuring dimensional quality: *irrecoverable*, *irreversible* and *reversible*. The *irrecoverable* category corresponds to (typically large) part deformations during handling that are catastrophic resulting in having to scrap the part and/or interrupt the operation of the material handling system. *Irrecoverable* part deformations need to be strictly avoided, including plastic deformations and part deformations that would result in collisions between the deformed part and obstacles in the workspace. These need to be anticipated for when formulating the constraint present in Eq. (5).

The *irreversible* category includes deformations that deteriorate the handled part's dimensional quality, such as deformations that contribute to nesting errors and part distortions, but do not lead to scrap or production interruptions [1]. It is proposed that this category of deformations needs to be minimised in order to find the optimal trade-off between the productivity (cycle-time) of the material handling system and the effect on the part's dimensional quality. In order to evaluate the improvements of the optimised trajectories with the proposed methodology in terms of ensuring the part's dimensional quality, further investigation is necessary to quantifying the relationship between on the one hand part deformation during handling and on the other hand nesting errors and part distortions.

The *reversible* category considers benign deformations that do not affect dimensional quality, plastic deformation, nor cause collisions between part and obstacles. Reversible deformations should not contribute to the value of the objective function in Eq.(16). For scenarios where any deterioration of part dimensional quality needs to be strictly avoided, it becomes necessary to determine the cycle-time threshold for which all deformations during handling are reversible. This corresponds to turning the constraint in Eq.(5) in an objective function and the objective function in Eq.(16) in a constraint. In this way, the pro-

posed methodology provides the productivity capability of the material handling system without any deterioration of dimensional quality.

8. Conclusions

This paper investigated trajectory optimisation for multi-robot systems that handle compliant parts in order to minimise the deformations during handling. The deformation of the handled parts is a critical issue in order to ensure the required final dimensional quality. A non-linear programming (NLP) model for multi-robot coordinated trajectory optimisation to minimise the deformations of the handled compliant parts is proposed. Part deformations are estimated by the proposed NLP optimisation model using a precomputed RSM based on data samples generated by FEA of the handled part and end-effector. The end-effectors' holding force, plastic part deformations, collision-avoidance and multi-robot coordination are considered as constraints in the model.

The resulting trajectories are validated on a real robot and evaluated compared to reference trajectories generated by the controller provided by the robot supplier. The proposed NLP model was applied in an industrial case-study with consideration to a multi-robot system for material handling tending in a sheet metal stamping press. The results of the performed tests show significant, up to 12 %, reduction in part deformations with the optimisation trajectories when compared to the reference trajectories. The cycle-time of the system remains the same such that the productivity is maintained. Results demonstrate the model is able to significantly reduce part deformations during handling, which reduces the risk of deteriorating the part's dimensional quality and improves the pick/place accuracy. This work addresses the current lack of approaches for systematically controlling or reducing deformations of compliant parts during handling which is often a critical issue for productivity and part quality in industrial manufacturing systems.

Acknowledgements

The authors thank Nima K. Nia and Volvo Cars Corporation for their support and industrial insights concerning material handling for sheet metal press lines.

This work was performed at the *Digital Lifecycle Management (DLM)* research group of *WMG* at the University of Warwick in Coventry (UK), and at University West's *Production Technology West (PTW)* research centre in Trollhättan (Sweden). Furthermore, this work is supported by *Västra Götalandsregionen* (Sweden), under the grant PROSAM+ RUN 612-0208-16. This study was also partially supported by the *UK EPSRC* project EP/K019368/1: *Self-Resilient Reconfigurable Assembly Systems with In-process Quality Improvement*.

References

[1] H. F. Li, D. Ceglarek, J. Shi, A dexterous part-holding model for handling compliant sheet metal parts, Journal of Manufacturing Science and Engineering 124 (1) (2002) 109–118.

[2] D. Ceglarek, H. F. Li, Y. Tang, Modeling and optimization of end effector layout for handling compliant sheet metal parts, Journal of Manufacturing Science and Engineering 123 (3) (2001) 473–480.

[3] H. Hoffmann, M. Kohnhuser, Strategies to Optimize the Part Transport in Crossbar Transfer Presses, CIRP Annals - Manufacturing Technology 51 (1) (2002) 27–32.

[4] H. Li, D. Ceglarek, Optimal Trajectory Planning For Material Handling of Compliant Sheet Metal Parts, Journal of Mechanical Design 124 (2) (2002) 213–222.

[5] S. Aomura, A. Koguchi, Optimized bending sequences of sheet metal bending by robot, Robotics and Computer-Integrated Manufacturing 18 (1) (2002) 29–39.

[6] J. Belchior, M. Guillo, E. Courteille, P. Maurine, L. Leotoing, D. Guines, Off-line compensation of the tool path deviations on robotic machining: Application to incremental sheet forming, Robotics and Computer-Integrated Manufacturing 29 (4) (2013) 58–69.

[7] D. Opritescu, W. Volk, Automated driving for individualized sheet metal part productionA neural network approach, Robotics and Computer-Integrated Manufacturing 35 (2015) 144–150.

[8] E. Glorieux, S. Riazi, B. Lennartson, Productivity/energy optimisation of trajectories and coordination for cyclic multi-robot systems, Robotics and Computer-Integrated Manufacturing 49 (2018) 152–161.

[9] A. M. Okamura, N. Smaby, M. R. Cutkosky, An overview of dexterous manipulation, in: Proceedings 2000 ICRA. Millennium Conference. IEEE International Conference on Robotics and Automation. Symposia Proceedings (Cat. No.00CH37065), Vol. 1, 2000, pp. 255–262 vol.1.

[10] A. Bicchi, V. Kumar, Robotic grasping and contact: a review, in: Proceedings 2000 ICRA. Millennium Conference. IEEE International Conference on Robotics and Automation. Symposia Proceedings (Cat. No.00CH37065), Vol. 1, 2000, pp. 348–353 vol.1.

[11] J. Butterfass, M. Grebenstein, H. Liu, G. Hirzinger, DLR-Hand II: next generation of a dextrous robot hand, in: Proceedings 2001 ICRA. IEEE International Conference on Robotics and Automation (Cat. No.01CH37164), Vol. 1, 2001, pp. 109–114 vol.1.

[12] D. Rus, M. T. Tolley, Design, fabrication and control of soft robots, Nature 521 (7553) (2015) 467–475.

[13] P. Jimnez, Survey on model-based manipulation planning of deformable objects, Robotics and Computer-Integrated Manufacturing 28 (2) (2012) 154–163.

[14] E. Glorieux, B. Svensson, F. Danielsson, B. Lennartson, Multi-objective constructive cooperative coevolutionary optimization of robotic press-line tending, Engineering Optimization 49 (10) (2017) 1685–1703.

[15] X. Liao, G. G. Wang, Evolutionary path planning for robot assisted part handling in sheet metal bending, Robotics and Computer-Integrated Manufacturing 19 (5) (2003) 425–430.

[16] E. Glorieux, P. Franciosa, D. Ceglarek, End-effector design optimisation and multi-robot motion planning for handling compliant parts, Structural and Multidisciplinary Optimization (2017) 1–14.

[17] O. C. Zienkiewicz, R. L. Taylor, The Finite Element Method: Basics v. 1, 5th Edition, Butterworth-Heinemann Ltd, Oxford ; Boston, 2000.

[18] D. R. Cooper, K. E. Rossie, T. G. Gutowski, An Environmental and Cost Analysis of Stamping Sheet Metal Parts, Journal of Manufacturing Science and Engineering 139. doi:10.1115/MSEC2016-8880.
URL `http://dx.doi.org/10.1115/MSEC2016-8880`

[19] A. Gasparetto, V. Zanotto, A technique for time-jerk optimal planning of robot trajectories, Robotics and Computer-Integrated Manufacturing 24 (3) (2008) 415–426.

[20] P. Franciosa, A. Das, D. Ceglarek, L. Bolognese, C. Marine, A. Mistry, Design synthesis methodology for dimensional management of assembly process with compliant non-ideal parts, in: Proceedings of Joint Conference on Mechanical, Design Engineering & Advanced Manufacturing, 2014.

[21] P. Tuleja, u. Åidlovsk, Unilateral Gripping with Active Vacuum Suction Cup: Calculation of Gripping Force and Number of Suction Cups, Tech. Rep. : Transfer inovci 29/2014, Technical University of Kosice, Slovakia (2014).

[22] G. Mantriota, A. Messina, Theoretical and experimental study of the performance of flat suction cups in the presence of tangential loads, Mechanism and Machine Theory 46 (5) (2011) 607–617.

[23] L. E. Kavraki, S. M. LaValle, Motion Planning, in: B. Siciliano, O. Khatib (Eds.), Springer Handbook of Robotics, Springer Berlin Heidelberg,

2008, pp. 109–131.

[24] R. H. Byrd, J. Nocedal, R. A. Waltz, Knitro: An Integrated Package for Nonlinear Optimization, in: G. D. Pillo, M. Roma (Eds.), Large-Scale Nonlinear Optimization, no. 83 in Nonconvex Optimization and Its Applications, Springer, 2006, pp. 35–59.

[25] E. Glorieux, F. Danielsson, B. Svensson, B. Lennartson, Constructive cooperative coevolutionary optimisation for interacting production stations, The International Journal of Advanced Manufacturing Technology 80 (1-4) (2015) 673–688.

[26] Binar Olofstrm AB, Binar Press Automation - UniFeeder (2014). URL http://shop.binarolofstrom.se.k34.itc.se/index.php?id_product=2&controller=product&id_lang=1

[27] R. Fourer, D. Gay, B. Kernighan, A Modeling Language for Mathematical Programming, Management Science 36 (5) (1990) 519–554.

[28] P. Franciosa, D. Ceglarek, VRM Simulation toolkit (2016). URL http://www2.warwick.ac.uk/fac/sci/wmg/research/manufacturing/downloads/

[29] P. Franciosa, D. Ceglarek, Hierarchical synthesis of multi-level design parameters in assembly system, CIRP Annals - Manufacturing Technology 64 (1) (2015) 149–152.

[30] P. Franciosa, S. Gerbino, D. Ceglarek, Fixture Capability Optimisation for Early-stage Design of Assembly System with Compliant Parts Using Nested Polynomial Chaos Expansion, Procedia CIRP 41 (2016) 87–92.

[31] E. Larsen, S. Gottschalk, M. C. Lin, D. Manocha, Fast Proximity Queries with Swept Sphere Volumes, in: Proc. IEEE Int. Conf. Robot. Autom, 2000, pp. 3719–3726.

[32] E. Glorieux, B. Svensson, F. Danielsson, B. Lennartson, Simulation-based Time and Jerk Optimisation for Robotic Press Tending, in: 29th European Simulation and Modelling Conference, EUROSIS, 2015, pp. 377–384.